

Simulation of the ion interactions for the ATIC experiment

H.J. Kim¹, S.K. Kim¹, T.Y. Kim¹, I.M. Koo¹, Y. Kwon¹, Y.J. Han¹, S.H. Lee¹, E.I. Won¹, O. Ganel²,
E.S. Seo², and J.Z. Wang²

For the ATIC Collaboration

¹Seoul National University, Seoul 151-742, Korea

²University of Maryland, College Park, MD, USA

Abstract

We have implemented event generators of relativistic ion interactions to a detector simulation package GEANT to understand the energy deposition and shower profile made by cosmic ions in the ATIC experiment. For 200 A · GeV/c Fe ion projectiles we observe a difference of about 10% in the mean energy deposition and get energy resolution of about 10-17% depending on the choice of the event generator. The difference can be attributed to the so called *spectator* fragmentation. The mean energy deposition in the calorimeter shows a linear dependence on the mass number and the incident energy per nucleon of the projectile ions for the range of 40 A · GeV/c to 200 A · GeV/c. The longitudinal and lateral shower profiles depend on the electromagnetic shower started by π^0 particles produced in the hadron interactions.

1 Introduction

The Advanced Thin Ionization Calorimeter (ATIC) will investigate the charge composition and energy spectra of primary cosmic rays over the energy range from about 10^{10} eV to about 10^{14} eV. The measurements of the differential energy spectrum are often summarized in a plot, which shows *the knee of the spectrum* between 10^{15} and 10^{16} eV (Gaisser T.K. et al., 1998). Recently a similar measurement by the JACEE collaboration based on the emulsion technique was reported (Asakimori K. et. al., 1998). A variety of models such as the supernova remnants model (SNR) have been proposed to explain the *knee*. The mass composition of cosmic rays are relevant to both origin and propagation, and specifically, the SNR model predicts a change in the mass composition around the knee. Hence, measurements of the composition and the energy spectra of the primary cosmic rays around the *knee* is of great importance (Erlykin and Wolfendale 1997). Heavy ion interactions in this range are also of interest, and they are under active study by accelerator based experiments at the BNL AGS (J. Barrette et al., 1999) and at the CERN SPS (Seyboth P. et al., 1999). The anti-centauro event reported by JACEE collaboration is a good example of such an interesting event (H. Wilczynski et al., 1997). The observation of these types of events has motivated many accelerator-based experiments. An experimental search for the $p + \bar{p}$ reaction showed a negative result (Bjorken J.D. et al., 1997). Experimental search for the ion interactions is being continued (Steinberg P. et al., 1998).

Measurement of the charge composition and energy spectra of primary cosmic rays in the planned range is the major goal of the experiment ATIC. While the latter subject includes many interesting possibilities, it also plays as the systematic uncertainty factor to the primary measurements. ATIC operates in the same region as JACEE but with a different measurement technique, and it is important to understand the systematic uncertainty caused by uncertainty in the ion interactions and the sensitivity of the detector to these uncertainties. For this goal, we have implemented the event generators of relativistic ion interactions to the detector simulation package GEANT (Brun. R. et al., 1994), and studied the systematic uncertainties in energy and shower profile measurements of ATIC for the energy range 40 A · GeV/c to 200 A · GeV/c, where an accelerator beam test is achievable.

2 Detector configuration and Observables

The detector includes the target module of about one proton interaction length and 2 radiation lengths, and the calorimeter module is composed of about 400 BGO crystals, each of which has approximate dimensions

of 2.5 cm by 2.5 cm by 25 cm. The crystals are arranged in 10 layers, and each layer has an area of 50 by 50 cm². The total thickness of the calorimeter is 25 cm corresponding to 22 radiation lengths and 1.1 interaction lengths (Seo et al.,1996). The 400 crystals are read independently, and the total deposited energy E_{tot} is obtained by the sum of the energy deposited in each crystal. Shower profiles are studied in units of the crystal thickness and widths.

3 Systematics in the particle production of the ion interactions

In the case of proton incidence, there is a considerable fraction of energy passing through the detector, as well as a large fluctuation of the energy deposited in the BGO calorimeter. The interaction point of the incident ion depends on the interaction cross section, which is often parametrized by $\sigma_{total} = 10\pi r_0^2 (A_t^{1/3} + A_p^{1/3} - \delta)$ where $r_0 \approx 1.35$ and $\delta \approx 1$ for the unit of mbarn (Westfall G.D. et al.,1979). For Fe projectiles, the interaction length is only about 7 cm, which is less than a fifth of the target thickness. Generally, the fluctuation in the first interaction point becomes less significant, but the violence of the collision becomes important for the ions. As the event generators of relativistic ion interactions, we selected the Relativistic Quantum Molecular Dynamics, RQMD (Sorge H. et al., 1989) and a dual parton model, DPMjetII (Ranft J., 1995). These models use different descriptions to simulate the ion interactions, but their predictions have been claimed to be consistent with experimental data (Gonin M. et al, 1995, J. Ranft, 1999).

We compare predictions of the models with data of the NA35 Collaboration (T. Alber et al., 1998) in Fig. 1 for the rapidity distribution of negatively charged particles h^- resulting from central S + S reactions at $200A \cdot GeV/c$. Both models show good agreement with the data but the DPMjetII model produces about 10% more particles than the RQMD model in the midrapidity region. Most of the h^- particles are composed of π^- particles, and the distribution of the π^- particles is close to that of π^0 and π^+ particles from isospin symmetry. For this reason, the rapidity distribution of the h^- 's is often used to discuss the degree of stopping of the projectile ion by the target nucleus (Seyboth P. et al., 1999). The rapidity distribution of the produced π^0 particles is closely related to the distribution of the angle of the produced π^0 particles. The models will be realistic in describing the electromagnetic component in the total energy deposited in the calorimeter and the shower profile, since the EM component is closely related to the π^0 production, as will be discussed later.

Baryons carry a large fraction of the energy after the ion interactions, so we also compared the lateral distribution of protons with the data of NA44 (Boggild H. et al., 1998). In this comparison, the DPMjetII model underpredicts the high m_t tail. This is due to the fact that the dual parton model is a multi-chain model, and the chains in p-p, p-A or A-A collisions have the same properties. Accordingly, the model can not reproduce the large change in the E_t distributions from the $p + p$ reaction to the central $A + A$ collisions, according to the author of the model. The present comparison was performed for the so-called *central interactions*, but a large fraction of ion interactions belong to the so-called *peripheral collision*. Baryons produced at 0 degree for

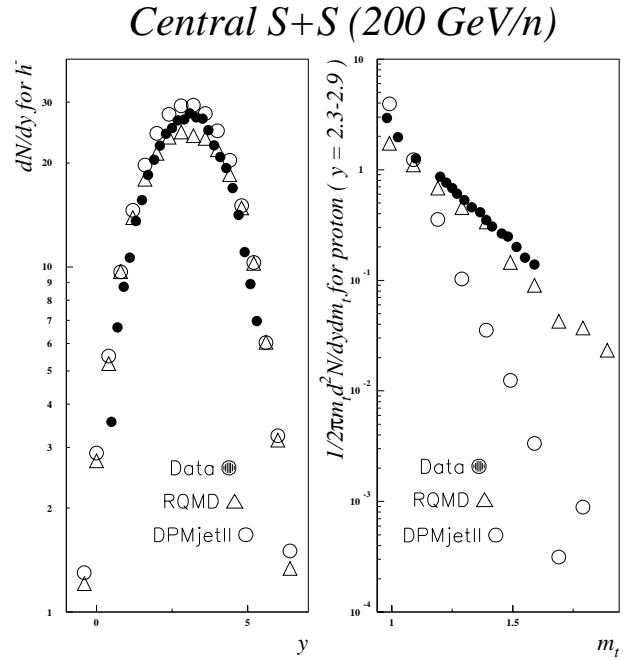


Figure 1: Comparison of the calculations by the event generators and the data for the central S+S reactions at $200A \cdot GeV/c$

peripheral collisions exist frequently as nuclei, rather than being individual nucleons (Ogilvie C.A. et al., 1996, Singh G. et al., 1994, 1996). The DPMjetII model includes a fragmentation model for the spectators for peripheral interactions (Ferrari A. et al., 1996). The RQMD model reports the spectators as individual nucleons, and we apply a simple coalescence model to those spectator nucleons to account for fragmentation of the spectator. In this case, most of the projectile spectator nucleons are coalesced to a nucleus.

4 Mean energy deposition and Shower profile

Figure 2 shows the total energy deposited in the BGO calorimeter when $200A \cdot GeV/c$ Fe ions make a normal incidence at the center of ATIC. Simulation using DPMjetII shows the larger E_{mean} , the mean energy deposition, by about 10%. The major difference between the two generators is the different treatment of the spectator fragmentation. Spectator fragmentation to smaller nuclei will effectively increase the number of hadron interactions, on average, and thereby increase the mean energy deposition. This reasoning is consistent with the fact that the total deposited energy shows larger fluctuations when the ion interactions are simulated using the RQMD model. More particle production at midrapidity will contribute only a minor fraction of the difference, since the central ion interaction is only a part of the interactions happening in ATIC.

The E_{mean} per nucleon is similar to that of the $200 GeV/c$ proton projectile. We inspected the linearity in E_{mean} for the oxygen (O) and iron (Fe) projectiles incident at $40 A \cdot GeV$ and $200 A \cdot GeV$. The inspection reveals a good linearity, better than 5%, with respect to mass number and the incident energy per nucleon of the projectile. The energy resolution, $\sigma(E)/E$, is about 10-17% depending on the choice of the generator when $200A \cdot GeV/c$ Fe ions are incident on ATIC. While E_{mean} shows a behaviour similar to the superposition of individual nucleons, the width of the E_{tot} distribution is considerably bigger than that expected from a simple superposition model. We believe fragmentation of the spectators plays an important role in determining the width of the distribution.

Figure 3 shows the shape of this shower development for a typical event simulated with the DPMjetII generator when $200A \cdot GeV/c$ Fe ions made a normal incidence on the center of ATIC. The longitudinal development of the shower in the BGO calorimeter can be reconstructed by summing the deposited energy in each layer of the calorimeter. The shower maximum appears mostly at the 3rd or 4th layer, corresponding to about 8 radiation length.

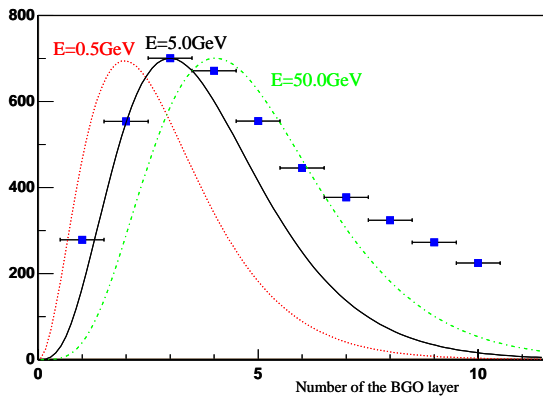


Figure 3: The typical shape of the deposited energy in the BGO calorimeter when $200A \cdot GeV/c$ Fe ions made a normal incidence on the ATIC at the center.

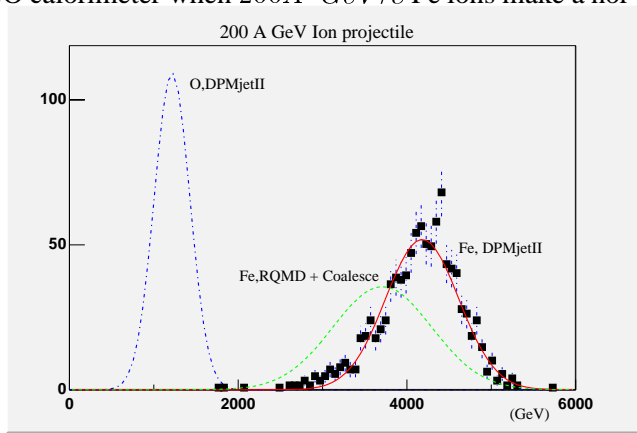


Figure 2: Total energy deposited in the BGO calorimeter

larger fluctuation in the position of the shower maximum. This behavior is consistent with the behavior of other observables, and we deduce that the fluctuation of

the interaction point of the secondary ions is an important element to be understood. The lateral development of the energy deposition in the BGO calorimeter is characterized by a narrow core with a wide tail and the root-mean-square of the distribution shows a minimum at the layer of the shower maximum. A large fraction of the deposited energy, more than 80% of the E_{tot} , is contained within the Molière radius at the shower max. This is similar to electromagnetic shower started by e or γ (Groom D.E., 1998). By projecting the produced π^0 's on to the surface of the BGO crystals, we observed the lateral development made by the kinematic distributions resulting from hadron interactions are only a small fraction of the R_M . We conclude that the lateral development of the shower is characterized by the electromagnetic shower started after the decay of the produced π^0 particles.

5 Conclusion and Outlook

By implementing the generators of relativistic ion interaction in the GEANT package, we have studied the systematic uncertainties and sensitivity of ATIC. Two selected event generators, the RQMD and the DPMjetII, show fair agreements with the measured data for h^- production, which is closely related to the energy deposited in the BGO calorimeter. We added a simple coalesce model to the RQMD model to account for *spectator* fragmentation, which differs from the DPMjetII model for the studied range. We address the difference as the possible source of the systematic difference in energy distribution and the longitudinal profile of the shower development between the two simulation results. With a beam test, we will be able to improve our understanding of the systematics. Measurement of relativistic ion interactions around $20 A \cdot TeV$ region will be made at the BNL RHIC in the near future (Nagamiya S. et al., 1993). The longitudinal development of showers in the BGO calorimeter is sensitive to secondary ion interactions, and the identification of an exotic event, such as the anticentauro event, remains as a possibility.

References

- Gaisser T.K. et. al., The European Physical Journal C3 (1998) 132-137.
 Asakimori K. et. al., ApJ 502 (1998) 278-283.
 Erlykin A.D., Wolfendale A.W., Astrop. Phys. 7 (1997) 1
 Barrette J. et al. Phys.Rev.C59 (1999) 884-888. as an example.
 Seyboth P. et al. Phys.Rev.Lett.82 (1999) 2471-2475. as an example.
 Wilczynski H. et al., Nucl. Phys. B (Proc. Suppl.) 52B (1997) 81-91.
 Bjorken J.D. et al., Phys.Rev. D55 (1997) 5667-5680.
 Steinberg P. et al., Phys.Lett. B420 (1998) 169-179.
 Nagamiya S. et al., PHENIX Conceptual Design Report (CDR), Presented at DOE/RHIC Review, BNL, January 1993 (Informal Report) ed. W.L. Kehoe. as an example
 Brun R. et al., GEANT, CERN Program Library Long Writeup W5013 (1994)
 Seo et al., SPIE Proceedings vol 286, Gamma-Ray and Cosmic Ray Detectors, Techniques, and Missions, pp134-144, 1996.
 Westfall G.D. et al., Phys. Rev. C19 (1979) 1309.
 Alber T. et al., Eur.Phys.J. C2 (1998) 643-659.
 Boggild H. et al., Phys.Rev. C57 (1998) 837-846.
 Sorge H. et al., Ann. Phys. (USA) 192 (1989) 266.
 Ranft J., Phys. Rev. D51 (1995) 64
 Gonin M. et al, Phys. Rev. C51 (1995) 310.
 Ranft. J., Nucl.Phys.Proc.Suppl. 71 (1999) 228-237
 Ogilvie C.A. et al., Nucl. Phys. A607 (1996) 457
 Singh G. et al., Phys. Rev. C54 (1996) 3185-3194., Phys. Rev. C50 (1994) 1085-1089
 Ferrari A. et al., Z.Phys. C71 (1996) 75-86
 Groom D.E., The European Physical Journal C3 (1998) 144-151.